THEORETICAL AND APPLIED MECHANICS
Volume 46 (2019) Issue 2, 125–145 DOI: https://doi.org/10.2298/TAM181120008S

INFLUENCE OF MICRO-ROTATION AND MICRO-INERTIA ON NANOFLUID FLOW OVER A HEATED HORIZONTAL CIRCULAR CYLINDER WITH FREE CONVECTION

Mohammed Z. Swalmeh, Hamzeh T. Alkasasbeh, Abid Hussanan, and Mustafa Mamat

Abstract. The addition of nanoparticles into conventional heat transfer fluids is one of the modern science techniques that offer better heat transfer performance. However, micropolar fluid model is not considered under these nanoparticles effects. Therefore, the main objective of this study is to explore the nanofluids to understand the microstructure and inertial characteristics of nanoparticles. In this paper, heat transfer flow of a micropolar nanofluid mixture containing copper (Cu) and silver (Ag) nanoparticles is investigated over a heated horizontal circular cylinder. The dimensionless governing equations are solved via an implicit finite difference scheme known as Keller-box method. The results of the nanofluid mixture are compared with those with a Newtonian fluid. The effects of different parameters on velocity, angular velocity and temperature are examined graphically for both Cu/Ag-water and Cu/Ag-kerosene oil. Results show that the heat transfer coefficient of the Cu/Ag-kerosene oil nanofluid mixture is larger than that of the Cu/Ag-water nanofluid, when comparison is based on a fixed value of the micro-rotation parameter.

1. Introduction

Micropolar fluids, a subclass of microfluids, are considered to be a special kind of suspensions described by micropolar theories. Eringen [1] was the first to introduce the theory of micropolar fluids, in which the stress tensor is no longer symmetric but rather an anti-symmetric characteristic due to the oriented micro-rotation of particles. There have been published several studies on the understanding of the development of micropolar theories and their applications [2]. Agarwal et al. [3] considered micropolar heat transfer flow past a stationary porous wall. Chemical reaction and heat absorption/generation effects on micropolar free convection flow over a stretched permeable surface were investigated by Rebhi et al. [4]. Bachok et al. [5] considered flow of a micropolar fluid over an unsteady stretching

2010 *Mathematics Subject Classification:* 76-XX; 76DXX; 76RXX; 80Axx.
Key words and phrases: microstructure, micropolar nanofluid, free convection, circular cylinder.

sheet. Unsteady MHD mixed convection periodic flow of a micropolar fluid with thermal radiation and chemical reaction was examined by Pal and Talukdar [6]. They used a perturbation technique as the main tool to obtain solutions analytically. Turkyilmazoglu [7] considered micropolar fluid heat transfer flow due to a porous stretching sheet. Micropolar forced convection flow a over moving surface under magnetic field was reported by Waqas et al. [8]. Micropolar fluid unsteady free convection flow over a vertical plate with Newtonian heating is considered by Hussanan et al. [9]. Hussanan et al. [10] obtained an exact solution of heat and mass transfer in micropolar fluid over an oscillating vertical plate under Newtonian heating effects. Alkasasbeh [11] presented the numerical solution for heat transfer magnetohydrodynamic flow of a micropolar casson fluid over a horizontal circular cylinder with thermal radiation using Keller-box method.

In past decades, different techniques have been used to improve the rate of heat transfer to reach a different level of thermal efficiencies. To achieve this object, the enhancement of thermal conductivity is very important. Choi [12] was the first who conducted research on enhancement of heat transfer in convectional fluids through suspended nanoparticles (with sizes significantly smaller than 100 nm). Nanofluids are a new type of working fluids containing uniformly dispersed and suspended metallic or nonmetallic nanoparticles. After the revolutionary work of Choi [12], this research topic has attracted the attention of many researchers due to its fascinating thermal characteristics and potential applications. Two mathematical models have been used to study the characteristics of nanofluids, namely Buongiorno model [13] and Tiwari-Das model [14]. Buongiorno approach focuses on Brownian diffusion and thermophoresis mechanisms. In view of its great importance, many authors have used this model in the analysis of nanofluid flow, for example, Noreen et al. [15]; Boulahia et al. [16]; Qasim et al. [17]; Wakif et al. [18]; Afridi and Qasim [19].

On the other hand, Tiwari-Das model considered nanoparticles volume fraction instead of Brownian motion and thermophoresis effects. In the recent years, some interesting results have been obtained by many researchers by using this model. The flow of water based nanofluids past a wedge with partial slip was analysed by Rahman et al. [20]. Sheremet et al. [21] considered thermal stratification on free convection in a square porous cavity filled with a nanofluid. Unsteady MHD flow of some nanofluids through a porous medium over an accelerated vertical plate was investigated by Hussanan et al. [22]. Chen et al. [23] performed the analysis of the nanofluid flow in a porous channel with suction and chemical reaction. Sheikholeslami [24] considered magnetic field on a water based nanofluid with an Fe_3O_4 nanoparticles. Sheikholeslami [25] continued with the same model and investigated the influence of coulomb forces on Fe_3O_4 suspended water based nanofluid in a cavity with a moving wall. Hussanan et al. [26] investigated the natural convection flow of a micropolar nanofluid over a vertical plate. They analyzed the impact of oxide nanoparticles on water, kerosene and engine oil based nanofluids. Flow of Casson sort of nanofluid over a vertical plate with leading edge accretion/ablation using sodium alginate as a base fluid has been considered by Hussanan [27]. Hussanan et al. [28] also studied the microstructure and inertial characteristics of a

magnetite ferrofluid using the micropolar fluid model. Swalmeh et al. [29] highlighted the impacts of natural convection on the boundary layer flow of Cu-water and Al_2O_3-water micropolar nanofluid about a solid sphere.

To the best of the authors' knowledge, the problem of the flow of a water and kerosene oil based micropolar nanofluid suspended by copper (Cu) and silver (Ag) over a heated horizontal circular cylinder has not been investigated by any researcher up till now. To fill out the gap, heat transfer flow of a micropolar nanofluid mixture containing copper and silver nanoparticles is considered over a heated horizontal circular cylinder. A similarity transformation is used to convert the governing equations into nonlinear ordinary differential equations, which are solved via an implicit finite difference scheme known as Keller-box method.

2. Mathematical analyses

Consider the free convection over a heated horizontal circular cylinder of radius a, which is immersed in a steady laminar two-dimensional incompressible and viscous micropolar nanofluid of copper (Cu) and silver (Ag) in two different types of base fluids, water and kerosene oil, in a prescribed wall temperature. In figure 1 the surface temperature of the cylinder is $T_w > T_\infty$, the ambient temperature of the fluid which remains unchanged, and the gravity vector g acts downward in the opposite direction, where $\bar{x}$-coordinate is measured along the circumference of the horizontal circular cylinder from the lower stagnation point, $\bar{y}$-coordinate is measured normal to the surface of the circular cylinder. Under these assumptions

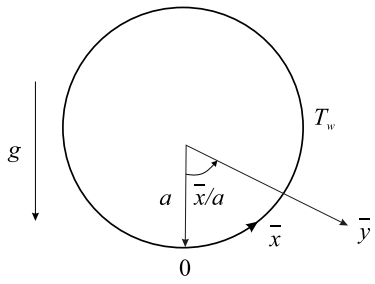

FIGURE 1. Physical model and coordinate system.

along with the Boussinesq approximation, the governing equations of a micropolar nanofluid with heat transfer are given by (see, Mansour et al. [32]; Abbas et al. [33]) as

$$\frac{\partial \bar{u}}{\partial \bar{x}} + \frac{\partial \bar{v}}{\partial \bar{y}} = 0, \tag{2.1}$$

$$\rho_{nf}\left(\bar{u}\frac{\partial \bar{u}}{\partial \bar{x}} + \bar{v}\frac{\partial \bar{v}}{\partial \bar{y}}\right) = (\mu_{nf} + \kappa)\frac{\partial^2 \bar{u}}{\partial \bar{y}^2} + \rho_{nf}(\chi\rho_s\beta_s + (1-\chi)\rho_f\beta_f)g(T - T_\infty)\sin\left(\frac{\bar{x}}{a}\right) + \kappa\frac{\partial \bar{H}}{\partial \bar{y}}, \tag{2.2}$$

$$\bar{u}\frac{\partial T}{\partial \bar{x}} + \bar{v}\frac{\partial T}{\partial \bar{y}} = \alpha_{nf}\frac{\partial^2 T}{\partial \bar{y}^2},$$

$$\rho_{nf} j\Big(\bar{u}\frac{\partial \bar{H}}{\partial \bar{x}} + \bar{v}\frac{\partial \bar{H}}{\partial \bar{y}}\Big) = -\kappa\Big(2\bar{H} + \frac{\partial \bar{u}}{\partial \bar{y}}\Big) + \phi_{nf}\frac{\partial^2 \bar{H}}{\partial \bar{y}^2}, \tag{2.3}$$

subject to the boundary conditions defined by Nazar et al. [30] as

$$\begin{aligned} &\bar{u} = \bar{v} = 0, \qquad T = T_w, \qquad \bar{H} = -\eta\frac{\partial \bar{u}}{\partial \bar{y}} \quad \text{at} \quad \bar{y} = 0,\\ &\bar{u} \to 0, \qquad T \to T_\infty, \qquad \bar{H} \to 0 \quad \text{as} \quad \bar{y} \to \infty \end{aligned} \tag{2.4}$$

where $\bar{u}$ and $\bar{v}$ are the velocity components along with the $\bar{x}$ and $\bar{y}$ axes, $j = \frac{a^2}{\sqrt{Gr}}$ is micro-inertia density. All the other symbols and quantities are shown in nomenclature. The ρ_{nf}, μ_{nf} and α_{nf} are density, viscosity and thermal diffusivity of a nanofluid, respectively, which are defined by Swalmeh et al. [29] as

$$\begin{aligned} \rho_{nf} &= (1-\chi)\rho_f + \chi\rho_f,\\ \mu_{nf} &= \frac{\mu_f}{(1-\chi)^{2.5}},\\ (\rho c_p)_{nf} &= (1-\chi)(\rho c_p)_f + \chi(\rho c_p)_s,\\ \frac{k_{nf}}{k_f} &= \frac{(k_s+2k_f) - 2\chi(k_f - k_s)}{(k_s+2k_f) + \chi(k_f - k_s)},\\ \alpha_{nf} &= \frac{k_{nf}}{(\rho c_p)_{nf}}, \end{aligned} \tag{2.5}$$

where χ is the nanoparticles volume fraction. In order to simplify the mathematical analysis of the problem, we introduce the following non-dimensional variables (Nazar et al. [30])

$$\begin{aligned} x = \frac{\bar{x}}{a}, \qquad y = Gr^{\frac{1}{4}}\Big(\frac{\bar{y}}{a}\Big), \qquad u = \Big(\frac{a}{\nu_f}\Big)Gr^{\frac{1}{2}}\bar{u}, \qquad v = \Big(\frac{a}{\nu_f}\Big)Gr^{\frac{1}{4}}\bar{v}\\ H = \Big(\frac{a^2}{\nu_f}\Big)Gr^{-3/4}\bar{H}, \qquad \theta = \frac{T - T_\infty}{T_w - T_\infty}, \end{aligned} \tag{2.6}$$

where $Gr = g\beta_f(T_w - T_\infty)a^3/{\nu_f}^2$ is the Grashof number for prescribed wall temperature conditions, and the spin gradient viscosity of nanofluid $\phi_{nf} = (\mu_{nf} + \frac{\kappa}{2})j$. Substituting equations (2.5) and (2.6) into equations (2.1) to (2.3), the following non-dimensional equations obtain

$$\frac{\partial u}{\partial x} + \frac{\partial v}{\partial y} = 0, \tag{2.7}$$

$$\begin{aligned} u\frac{\partial u}{\partial x} + v\frac{\partial u}{\partial y} = \frac{\rho_f}{\rho_{nf}}(D(\chi) + K)\frac{\partial^2 u}{\partial y^2}\\ + \frac{1}{\rho_{nf}}\Big(\chi\rho_s\Big(\frac{\beta_s}{\beta_f}\Big) + (1-\chi)\rho_f\Big)\theta\sin x + \frac{\rho_f}{\rho_{nf}}K\frac{\partial H}{\partial y}, \end{aligned} \tag{2.8}$$

$$u\frac{\partial\theta}{\partial x}+v\frac{\partial\theta}{\partial y}=\frac{1}{\Pr}\left[\frac{\frac{k_{nf}}{k_f}}{(1-\chi)+\chi\frac{(\rho c_p)_s}{(\rho c_p)_f}}\right]\frac{\partial^2\theta}{\partial y^2},$$

$$u\frac{\partial H}{\partial x}+v\frac{\partial H}{\partial y}=-\frac{\rho_f}{\rho_{nf}}K\Big(2H+\frac{\partial u}{\partial y}\Big)+\frac{\rho_f}{\rho_{nf}}\Big(D(\chi)+\frac{K}{2}\Big)\frac{\partial^2 H}{\partial y^2}, \tag{2.9}$$

where $K=\frac{\kappa}{\mu_f}$ is the micro-rotation parameter, $\Pr=\frac{v_f}{\alpha_f}$ is the Prandtl number and $D(\chi)=(1-\chi)^{-2.5}$. The boundary condition (2.4) becomes

$$\begin{aligned} &u=v=0, \qquad \theta=1, \qquad H=-\frac{1}{2}\frac{\partial u}{\partial y} \quad \text{at} \quad y=0,\\ &u\to 0, \qquad \theta\to 0, \qquad H\to 0 \quad \text{as} \quad y\to\infty. \end{aligned} \tag{2.10}$$

To solve equations (2.7) to (2.9), subject to the boundary conditions (2.10), we assume the following variables

$$\psi=xf(x.y), \quad \theta=\theta(x,y), \quad H=xh(x,y),$$

where ψ is the stream function defined as

$$u=\frac{\partial\psi}{\partial y}, \quad \text{and} \quad v=-\frac{\partial\psi}{\partial x},$$

which satisfies the continuity equation (2.7). Thus equations (2.8) to (2.9) become

$$\begin{aligned} &\frac{\rho_f}{\rho_{nf}}(D(\chi)+K)\frac{\partial^3 f}{\partial y^3}+f\frac{\partial^2 f}{\partial y^2}-\Big(\frac{\partial f}{\partial y}\Big)^2\\ &+\frac{1}{\rho_{nf}}\Big(\chi\rho_s\Big(\frac{\beta_s}{\beta_f}\Big)+(1-\chi)\rho_f\Big)\frac{\sin x}{x}\theta+\frac{\rho_f}{\rho_{nf}}K\frac{\partial h}{\partial y}=x\Big(\frac{\partial f}{\partial y}\frac{\partial^2 f}{\partial x\partial y}-\frac{\partial f}{\partial x}\frac{\partial^2 f}{\partial y^2}\Big), \end{aligned} \tag{2.11}$$

$$\frac{1}{\Pr}\left[\frac{k_{nf}/k_f}{(1-\chi)+\chi\frac{(\rho c_p)_s}{(\rho c_p)_f}}\right]\frac{\partial^2\theta}{\partial y^2}+f\frac{\partial\theta}{\partial y}=x\Big(\frac{\partial f}{\partial y}\frac{\partial\theta}{\partial x}-\frac{\partial f}{\partial x}\frac{\partial\theta}{\partial y}\Big),$$

$$\frac{\rho_f}{\rho_{nf}}\Big(D(\chi)+\frac{K}{2}\Big)\frac{\partial^2 h}{\partial y^2}+f\frac{\partial h}{\partial y}-\frac{\partial f}{\partial y}h-\frac{\rho_f}{\rho_{nf}}K\Big(2h+\frac{\partial^2 f}{\partial y^2}\Big)=x\Big(\frac{\partial f}{\partial y}\frac{\partial h}{\partial x}-\frac{\partial f}{\partial x}\frac{\partial h}{\partial y}\Big), \tag{2.12}$$

and boundary conditions

$$\begin{aligned} &f=\frac{\partial f}{\partial y}=0, \qquad \theta=1, \qquad h=-\frac{1}{2}\frac{\partial^2 f}{\partial y^2} \quad \text{at} \quad y=0,\\ &\frac{\partial f}{\partial y}\to 0, \qquad \theta\to 0, \qquad h\to 0 \quad \text{as} \quad y\to\infty. \end{aligned} \tag{2.13}$$

It can be seen that at the lower stagnation point of the sphere ($x\approx 0$), the above equations reduce to the following ordinary differential equations

$$\begin{aligned} &\frac{\rho_f}{\rho_{nf}}(D(\chi)+K)f'''+ff''-\Big(\frac{\partial f}{\partial y}\Big)^2\\ &\qquad+\frac{1}{\rho_{nf}}\Big(\chi\rho_s\Big(\frac{\beta_s}{\beta_f}\Big)+(1-\chi)\rho_f\Big)\theta+\frac{\rho_f}{\rho_{nf}}K\frac{\partial h}{\partial y}=0, \end{aligned} \tag{2.14}$$

$$\frac{1}{\Pr}\left[\frac{k_{nf}/k_f}{(1-\chi)+\chi\frac{(\rho c_p)_s}{(\rho c_p)_f}}\right]\theta''+f\theta'=0,$$

$$\frac{\rho_f}{\rho_{nf}}\Big(D(\chi)+\frac{K}{2}\Big)h''+fh'-\frac{\partial f}{\partial y}h-\frac{\rho_f}{\rho_{nf}}K(2h+f'')=0. \tag{2.15}$$

The boundary conditions become

$$\begin{aligned} &f(0)=f'(0)=0, && \theta(0)=1, && h(0)=-\frac{1}{2}f''(0) \quad \text{as} \quad y=0,\\ &f'\to 0, && \theta\to 0, && h\to 0 \quad \text{as} \quad y\to\infty, \end{aligned}$$

where primes denote differentiation with respect to y. The physical quantities of interest are the local skin friction coefficient C_f and the Nusselt number N_u, which can be written as

$$C_f=\frac{Gr^{-3/4}a^2}{\mu_f\nu_f}\tau_w, \quad N_u=\frac{aGr^{\frac{1}{4}}}{k_f(T_w-T_\infty)}q_w,$$

where

$$\tau_w=\Big(\mu_{nf}+\frac{\kappa}{2}\Big)\Big(\frac{\partial\bar{u}}{\partial\bar{y}}\Big)_{\bar{y}=0}, \quad q_w=-k_{nf}\Big(\frac{\partial T}{\partial\bar{y}}\Big)_{\bar{y}=0}.$$

By using the non-dimensional variables (2.6) and boundary conditions (2.10) the local skin friction coefficient C_f and Nusselt number N_u become

$$C_f=\Big(D(\chi)+\frac{K}{2}\Big)x\frac{\partial^2 f}{\partial y^2}(x,0), \quad N_u=-\frac{k_{nf}}{k_f}\Big(\frac{\partial\theta}{\partial y}\Big)(x,0).$$

3. Numerical solution

Equations (2.11) to (2.12) subject to boundary conditions (2.13) are solved numerically using the Keller-box method. This method seems to be the most flexible of the common methods and, despite recent developments in other numerical methods, remains a powerful and very accurate approach for parabolic boundary layer flows. It is also easily adaptable to solve equations of any order and unconditionally stable on the solutions. The solution is obtained by the following four steps

(i) Reduce the transformed equations (2.11) to (2.12) to a first-order system.
(ii) Write the difference equations using central differences.
(iii) Linearize the resulting algebraic equations by Newton's method and write them in matrix- vector form.
(iv) Solve the linear system by the block tridiagonal elimination technique. The numerical calculation displays that the boundary layer attains the top of the cylinder ($x=\pi$) without separating. Moreover, the step size for position x is chosen as $\Delta=\pi/6$ and the time step $\Delta x=0.005$ is sufficient to provide accurate numerical results and at ($x=\pi$), the boundary layer has non-zero thickness. Therefore, the boundary layer on each side of the cylinder must collide at ($x=\pi$) and leave the surface to form a thin buoyant plume above the cylinder.

4. Results and discussion

The natural convection boundary layer flow of micropolar nanofluids is inspected in a horizontal circular cylinder with a prescribed wall temperature. Two types of nanoparticles such as copper and silver are suspended in two different types of based fluids such as water and kerosene oil. The governing equations have been solved by Keller-box method and the results are shown in plots for different parameters such as micro-rotation parameter K and nanoparticle volume fraction χ on Nusselt number N_u, skin friction coefficient C_f, temperature, velocity and angular velocity fields. The numerical results of nonlinear partial differential equations start at the lower stagnation point of the sphere $x \approx 0$ with initial profiles as given by equations (2.14) to (2.15), and proceed round the circular cylinder up to $x = 180°$. Thermo-physical properties of based fluids and nanoparticles are given in Table 1. Tables 2 and 3 present the comparison values with the previous published results reported by Nazar et al. [30] and Merkin [31]. We have found that the present results are in a good agreement.

TABLE 1. Thermo-physical properties of based fluids and nanoparticles

Physical properties $\rho(kg/m^3)$	Water 997.1	Kerosene oil 783	Cu 8933	Ag 10500
$C_p(J/kg–K)$	4179	2090	385	235
$K(W/m–K)$	0.613	0.145	400	429
$\beta \times 10^{-5}(K^{-1})$	21	99	1.67	1.89
Pr	6.2	21	–	–

TABLE 2. Comparison of local Nusselt number N_u4 with viscous Newtonian fluid, when $\Pr = 1$, $K = 0$ and $\chi = 0$.

x	Nazar et al. [30]	Merkin [31]	Present
0°	0.4214	0.4214	0.4214
30°	0.4161	0.4161	0.4163
60°	0.4005	0.4007	0.4006
90°	0.3741	0.3745	0.3744
120°	0.3355	0.3364	0.3356
150°	0.2811	0.2825	0.2811
180°	0.1916	0.1945	0.1913

The impact of nanoparticle volume fraction χ and micro-rotation parameter K on the local Nusselt number and local skin friction for different values of x for a Cu/Ag nanoparticles water and kerosene oil based nanofluid are displayed in Figures 2 to 5. According to these figures, the kerosene oil based nanofluid with Cu/Ag nanoparticles has a higher local Nusselt number than the water based nanofluid with the same nanoparticles. However, the local skin friction of the

TABLE 3. Comparison of local skin friction coefficient C_f with viscous Newtonian fluid, when $\Pr = 1$, and $\chi = 0$.

x	Nazar et al. [30]	Merkin [31]	Present
0°	0.0000	0.0000	0.0000
30°	0.4148	0.4151	0.4159
60°	0.7542	0.7558	0.7538
90°	0.9545	0.9579	0.9574
120°	0.9698	0.9756	0.9743
150°	0.7740	0.7822	0.7813
180°	0.3265	0.3391	0.3311

Cu/Ag water based nanofluid is higher than the Cu/Ag kerosene oil based nanofluid whatever the values of the nanoparticle volume fraction χ. Further, it is also observed from these figures that the local Nusselt number and local skin friction are decreased with increasing the values of nanoparticles volume fraction χ and micro-rotation parameter K. Figures 6 to 8 illustrate the effect of nanoparticles volume fraction χ on temperature, velocity and angular velocity profiles for the Ag-water and Ag-kerosene oil based nanofluids. It is noted that as nanoparticles volume fraction χ increases, the values of both temperature and velocity profiles increase, while the angular velocity profiles decrease. Figures 9 to 11 depict the results of temperature, velocity and angular velocity profiles for the Ag-water and Ag-kerosene oil based nanofluids with various values of micro-rotation parameter K. As micro-rotation parameter K increases, the temperature and velocity profiles decrease, whereas angular velocity profiles increase. Figures 12 to 17 display the results of temperature, velocity, and angular velocity profiles of Cu and Ag in kerosene oil based nanofluids, respectively, with various values of nanoparticles volume fraction χ and micro-rotation parameter K. The temperature and velocity of both Cu and Ag in kerosene oil based nanofluids increase with higher values of nanoparticles volume fraction χ and this rise in temperature profiles is more common in the Ag-kerosene oil based nanofluid than the Cu-kerosene oil based nanofluid. It is also noted that the angular velocity of Cu-kerosene oil is significantly increased as compared to Ag-kerosene oil. On the other hand, the temperature increases with increasing values of micro-rotation parameter K and also velocity increases with an increase in micro-rotation parameter K. It is also noticed that the angular velocity decreases for higher values of micro-rotation parameter K.

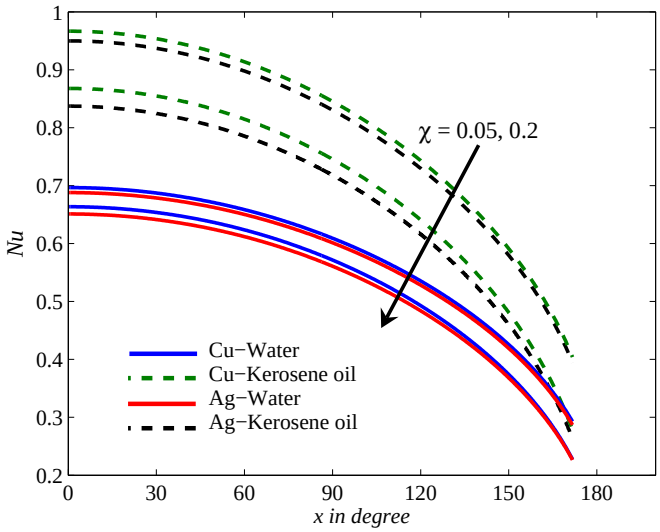

FIGURE 2. Variation of local Nusselt number of Cu/Ag in water and kerosene oil based nanofluids for various values of x and χ, when $K = 0.3$.

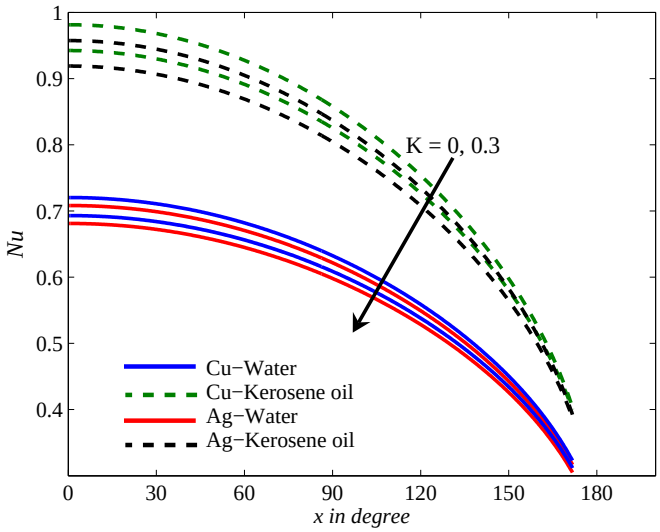

FIGURE 3. Variation of local skin friction of Cu/Ag in water and kerosene oil based nanofluids for various values of x and χ, when $K = 0.3$.

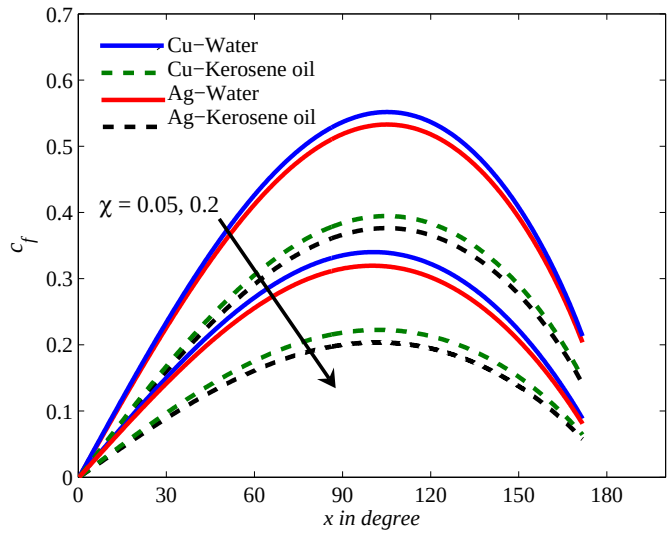

FIGURE 4. Variation of local Nusselt number of Cu/Ag in water and kerosene oil based nanofluids for various values of x and K, when $\chi = 0.1$.

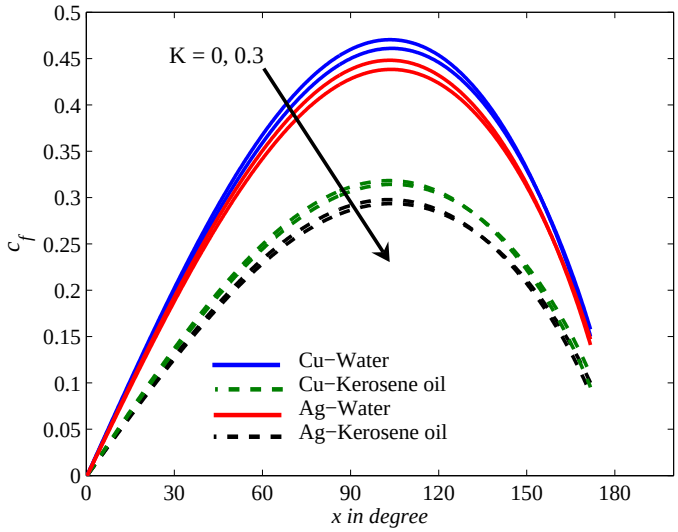

FIGURE 5. Variation of local skin friction of Cu/Ag in water and kerosene oil based nanofluids for various values of x and K, when $\chi = 0.1$.

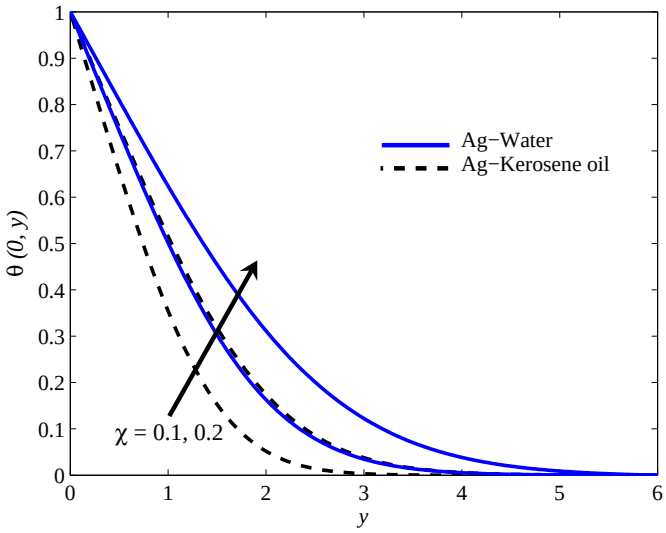

FIGURE 6. Variation of temperature field for Ag water and kerosene oil based nanofluids for various values of χ, when $K = 0.2$.

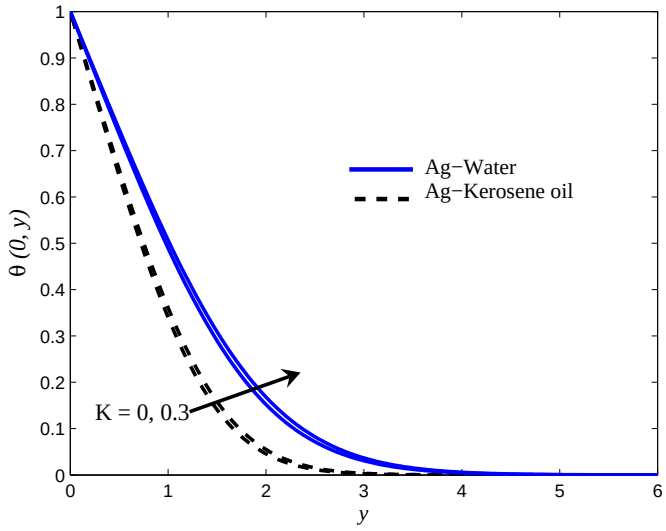

FIGURE 7. Variation of velocity field for Ag water and kerosene oil based nanofluids for various values of χ, when $K = 0.2$.

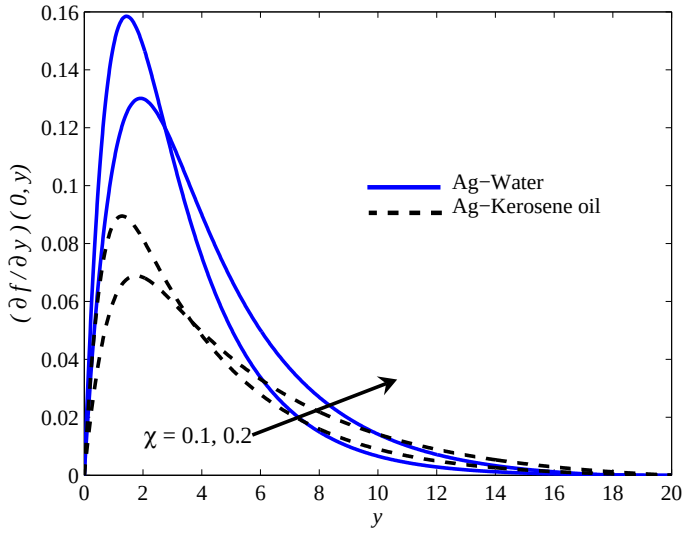

FIGURE 8. Variation of angular velocity field for Ag water and kerosene oil based nanofluids for various values of χ, when $K = 0.2$.

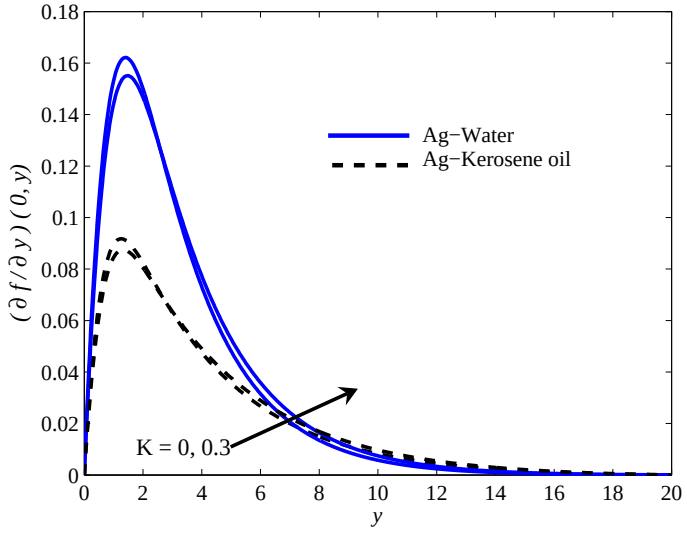

FIGURE 9. Variation of temperature field for Ag water and kerosene oil based nanofluids for various values of K, when $\chi = 0.1$.

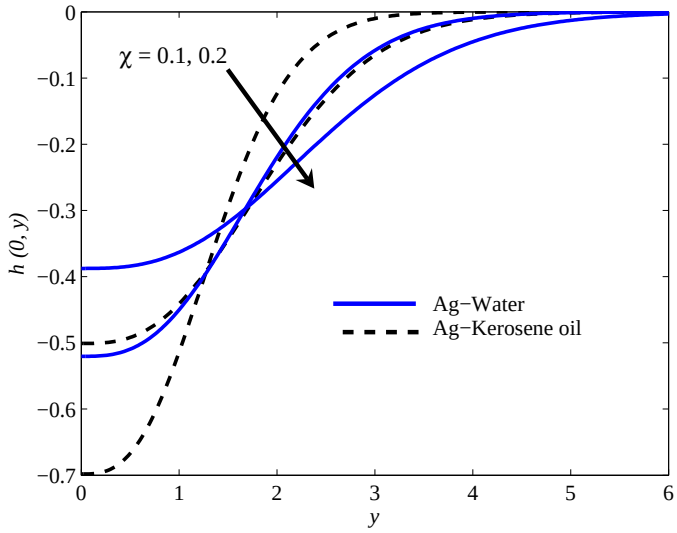

FIGURE 10. Variation of velocity field for Al_2O_3 water and kerosene oil based nanofluids for various values of K, when $\chi = 0.1$.

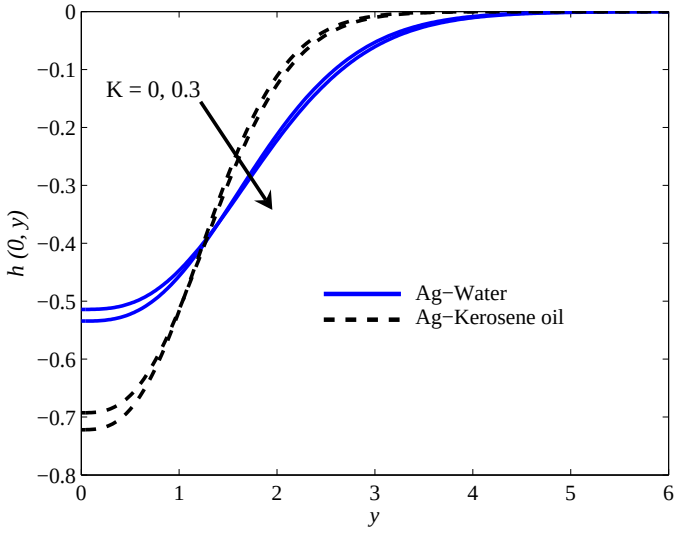

FIGURE 11. Variation of angular velocity field for Ag water and kerosene oil based nanofluids for various values of K, when $\chi = 0.1$.

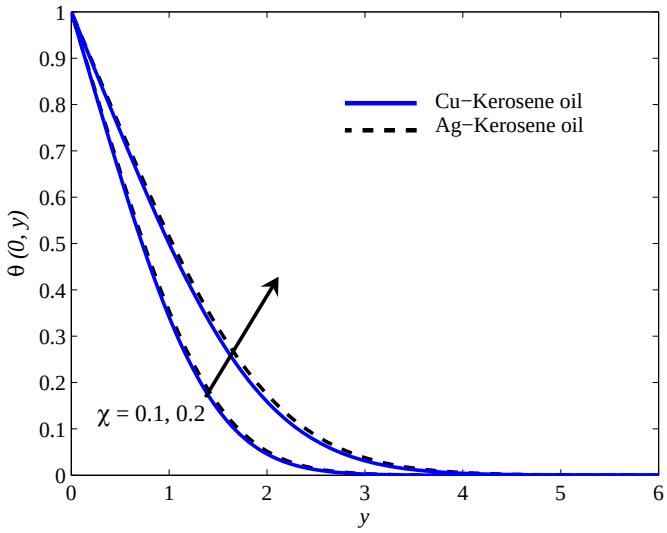

FIGURE 12. Variation of the temperature field for Cu/Al_2O_3-kerosene oil based nanofluid with various values of χ, when $K = 0.2$.

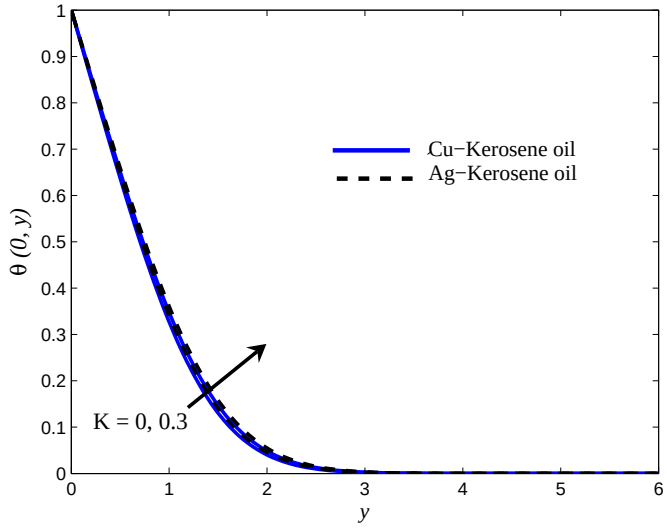

FIGURE 13. Variation of the velocity field for Cu/Al_2O_3-kerosene oil based nanofluid with various values of χ, when $K = 0.2$.

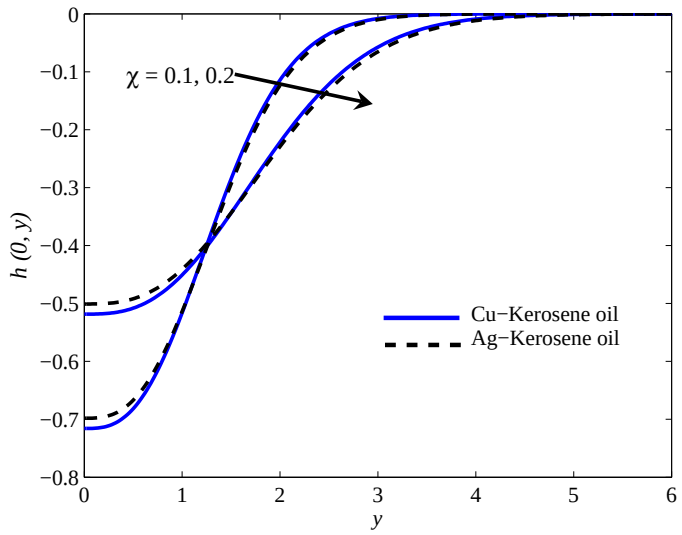

FIGURE 14. Variation of the angular velocity field for Cu/Al_2O_3-kerosene oil based nanofluid with various values of χ, when $K = 0.2$.

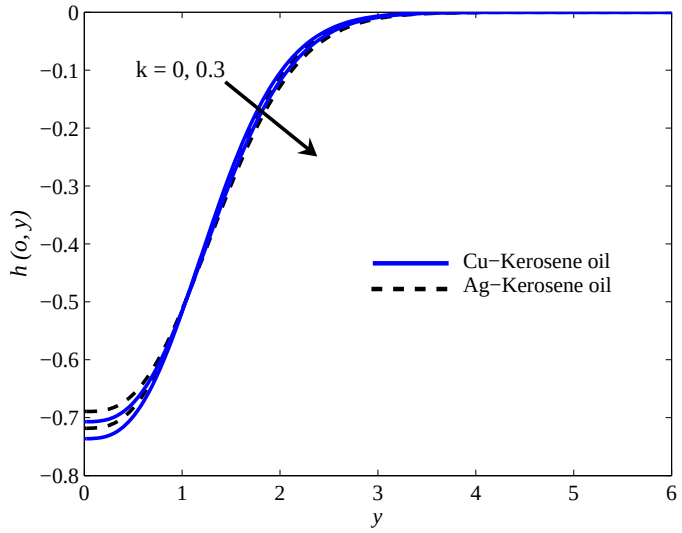

FIGURE 15. Variation of the temperature field for Cu/Al_2O_3-kerosene oil based nanofluid with various values of K, when $\chi = 0.1$.

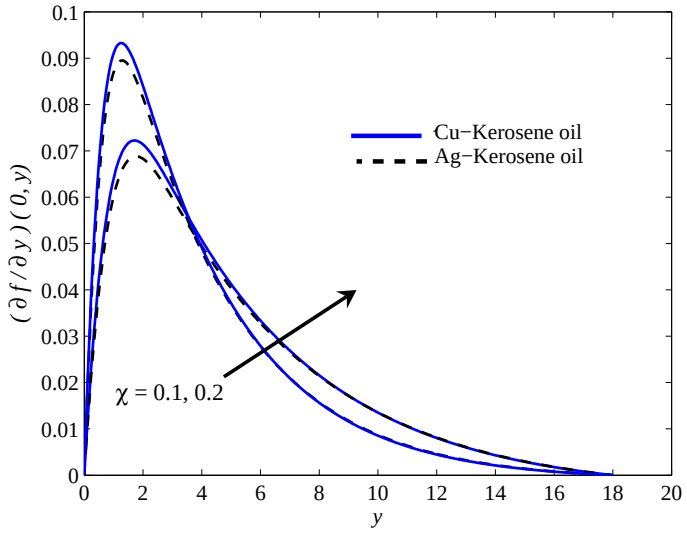

FIGURE 16. Variation of the velocity field for Cu/Al_2O_3-kerosene oil based nanofluid with various values of K, when $\chi = 0.1$.

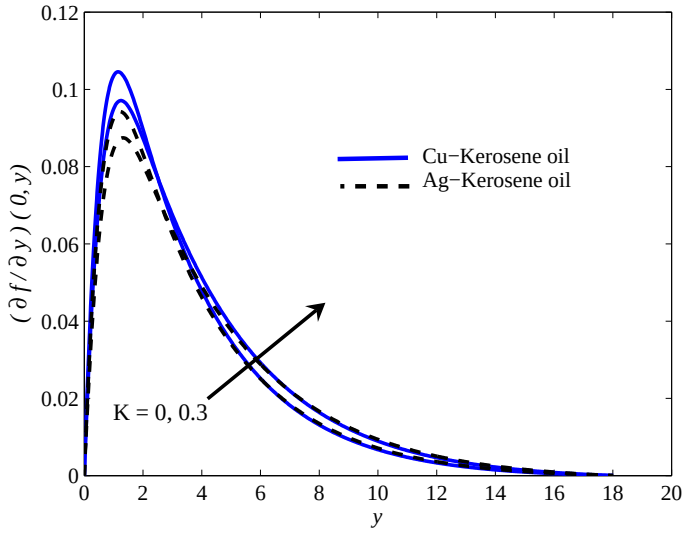

FIGURE 17. Variation of the angular velocity field for Cu/Al_2O_3-kerosene oil based nanofluid with various values of K, when $\chi = 0.1$.

5. Conclusions

In this paper, we have studied the problem of natural convection boundary layer flow on a horizontal circular cylinder immersed in a micropolar nanofluid with a prescribe wall temperature. We have sought to determine the effect of micro-rotation K and nanoparticles volume fraction χ of both copper Cu and silver Ag with two different types of based fluids, namely water and kerosene oil, which have been observed by using the suitable models for effective thermal conductivity and nanoparticles. Solutions of the governing non-similar equations are obtained numerically by Keller-box method. We can draw the following conclusions:

(i) Cu/Ag-kerosene oil has a higher local Nusselt number N_u if compared with Cu/Ag-water. Moreover Cu/Ag-kerosene oil has a lower local skin friction coefficient C_f compared with Cu/Ag-water.

(ii) Ag-water has a higher value of temperature and velocity profiles compared to Ag-kerosene oil, but the opposite happens in the case of angular velocity profiles for Ag-kerosene oil.

(iii) The value of temperature and velocity profiles for Ag have higher values than Cu based kerosene oil, but the different case of angular velocity profiles for Cu have higher values than Ag based kerosene oil.

(iv) When the nanoparticles volume fraction χ and micro-rotation parameter K increase, the temperature and velocity increase and decrease in angular velocity profiles.

6. Symbol

Table 4. Nomenclature

$c_{p,nf}$	Nanofluid heat capacity $[J \cdot kg^{-1} \cdot K^{-1}]$
g	Acceleration due to gravity $\left[m \cdot s^{-2}\right]$
Gr	Grashof number
j	Micro-inertia density $\left[m^2\right]$
K	Micro-rotation parameter
k_f	Base fluid thermal conductivity $\left[W \cdot m^{-1} \cdot K^{-1}\right]$
k_s	Solid particles thermal conductivity $\left[W \cdot m^{-1} \cdot K^{-1}\right]$
k_{nf}	Nanofluid thermal conductivity $\left[W \cdot m^{-1} \cdot K^{-1}\right]$
$\bar{H}$	Angular velocity $\left[m \cdot s^{-1}\right]$
Pr	Prandtl number
T	Temperature of the fluid $[K]$
T_w	Wall temperature $[K]$
T_∞	Ambient temperature $[K]$
u	$x-$ component of velocity $\left[m \cdot s^{-1}\right]$
v	$y-$ component of velocity $\left[m \cdot s^{-1}\right]$

TABLE 5. Greek symbols

α_{nf}	Nanofluid thermal diffusivity $\left[m^2 \cdot s^{-1}\right]$
χ	Nanoparticles volume fraction
κ	Vortex viscosity $\left[kg \cdot m^{-1} \cdot s^{-1}\right]$
μ_f	Base fluid dynamic viscosity $\left[kg \cdot m^{-1} \cdot s^{-1}\right]$
μ_{nf}	Nanofluid dynamic viscosity $\left[kg \cdot m^{-1} \cdot s^{-1}\right]$
ρ_f	Base fluid density $\left[kg \cdot m^{-3}\right]$
ρ_s	Solid particles density $\left[kg \cdot m^{-3}\right]$
ρ_{nf}	Nanofluid density $\left[kg \cdot m^{-3}\right]$
β_f	Base fluid thermal expansion coefficient $\left[K^{-1}\right]$
β_s	Solid particles thermal expansion coefficient $\left[K^{-1}\right]$
ϕ_{nf}	Spin gradient viscosity $\left[kg \cdot m \cdot s^{-1}\right]$
ψ	Stream function
θ	Dimensionless temperature

TABLE 6. Subscripts

f	Base fluid
s	Solid particles
nf	Nanofluid
w	Condition at wall
∞	Condition at infinity

Acknowledgments. The corresponding author would like to thank Ton Duc Thang University, Ho Chi Minh City, Vietnam for the financial support.

References

1. A. C. Eringen, *Theory of micropolar fluids*, J. Appl. Math. Mech. **16** (1966), 1–18.
2. K. Kumari, G. Nath, *Unsteady self-similar stagnation point boundary layers for micropolar fluids*, Indian Journal of Pure and Applied Mathematics **17**(2) (1986), 231–244.
3. R. S. Agarwal, R. Bhargava, A. V. S. Balaji, *Numerical solution of flow and heat transfer of a micropolar fluid at a stagnation point on a porous stationary wall*, Indian Journal of Pure and Applied Mathematics **21** (1990), 567–573.
4. A. D. Rebhi, M. Q. Al-Odat, J. C. Ali, A. S. Benbella, *Combined effect of heat generation or absorption and first-order chemical reaction on micropolar fluid flows over a uniformly stretched permeable surface*, International Journal of Thermal Sciences **48**(8) (2009), 1658–1663.
5. N. Bachok, A. Ishak, R. Nazar, *Flow and heat transfer over an unsteady stretching sheet in a micropolar fluid*, Meccanica **46** (2011), 935–942.
6. D. Pal, B. Talukdar, *Perturbation technique for unsteady MHD mixed convection periodic flow, heat and mass transfer in micropolar fluid with chemical reaction in the presence of thermal radiation*, Central European Journal of Physics **10**(5) (2012), 1150–1167.
7. M. Turkyilmazoglu, *Flow of a micropolar fluid due to a porous stretching sheet and heat transfer*, Int. J. Non-Linear Mech. **83** (2016), 59–64.
8. H. Waqas, S. Hussain, H. Sharif, S. Khalid, *MHD forced convective flow of micropolar fluids past a moving boundary surface with prescribed heat flux and radiation*, British Journal of Mathematics and Computer Science **21** (2017), 1–14.

9. A. Hussanan, M. Z. Salleh, I. Khan, R. M. Tahar, *Unsteady free convection flow of a micropolar fluid with Newtonian heating: closed form solution*, Thermal Science **21** (2017), 2307–2320.
10. A. Hussanan, M. Z. Salleh, I. Khan, R. M. Tahar, *Heat and mass transfer in a micropolar fluid with Newtonian heating: An exact analysis*, Neural Comput. Appl. **29** (2018), 59–67.
11. H. Alkasasbeh, *Numerical solution on heat transfer magnetohydrodynamic flow of micropolar Casson fluid over a horizontal circular cylinder with thermal radiation*, Frontiers in Heat and Mass Transfer **10** (2018), 1–7.
12. S. U. S. Choi, *Enhancing thermal conductivity of fluids with nanoparticles*, ASME International Mechanical Engineering Congress and Exposition **231** (1995), 99–105.
13. J. Buongiorno, *Convective transport in nanofluids*, ASME Journal of Heat Transfer **128** (2006), 240–250.
14. R. K. Tiwari, M. K. Das, *Heat transfer augmentation in a two-sided lid-driven differentially heated square cavity utilizing nanofluids*, International Journal of Heat and Mass Transfer **50** (2007), 2002–2018.
15. S. Noreen, M. M. Rashidi, M. Qasim, *Blood flow analysis with considering nanofluid effects in vertical channel*, Applied Nanoscience **7** (2017), 193–199.
16. Z. Boulahia, A. Wakif, R. Sehaqui, *Finite volume analysis of free convection heat transfer in a square enclosure filled by a Cu-water nanofluid containing different shapes of heating cylinder*, Journal of Nanofluids **6** (2017), 1–8.
17. M. Qasim, Z. H. Khan, I. Khan, Q. M. Al-Mdallal, *Analysis of entropy generation in flow of methanol-based nanofluid in a sinusoidal wavy channel*, Entropy **19** (2017), 490.
18. A. Wakif, Z. Boulahia, R. Sehaqui, *A semi-analytical analysis of electro-thermo-hydrodynamic stability in dielectric nanofluids using Buongiorno's mathematical model together with more realistic boundary conditions*, Results in Physics **9** (2018), 1438–1454.
19. M. I. Afridi, M. Qasim, *Comparative study and entropy generation analysis of Cu-H_2O and Ag-H_2O nanofluids flow over a slendering stretching surface*, Journal of Nanofluids **7** (2018), 783–790.
20. M. M. Rahman, M. A. Al-Lawatia, I. A. Eltayeb, N. Al-Salti, *Hydromagnetic slip flow of water based nanofluids past a wedge with convective surface in the presence of heat generation (or) absorption*, International Journal of Thermal Sciences **57** (2012), 172–182.
21. M. A. Sheremet, S. Dinarvand, I. Pop, *Effect of thermal stratification on free convection in a square porous cavity filled with a nanofluid using Tiwari and Das' nanofluid model*, Physica E **69** (2015), 332–341.
22. A. Hussanan, I. Khan, H. Hashim, M. K. A. Mohamed, N. Ishak, N. M. Sarif, M. Z. Salleh, *Unsteady MHD flow of some nanofluids past an accelerated vertical plate embedded in a porous medium*, Jurnal Teknologi **78** (2016), 121–126.
23. H. Chen, T. Xiao, M. Shen, *Nanofluid flow in a porous channel with suction and chemical reaction using Tiwari and Das's nanofluid model*, Heat Transfer–Asian Research, **45**(7) (2017), 1041–1052.
24. M. Sheikholeslami,(2016) *Magnetic source impact on nanofluid heat transfer using CVFEM*, Computing and Applications, DOI 10.1007/s00521-016-2740-7.
25. M. Sheikholeslami, *Influence of Coulomb forces on Fe_3O_4-H_2O nanofluid thermal improvement*, International Journal of Hydrogen Energy **42** (2017), 821–829.
26. A. Hussanan, M. Z. Salleh, I. Khan, S. Shafie, *Convection heat transfer in micropolar nanofluids with oxide nanoparticles in water, kerosene and engine oil*, Journal of Molecular Liquids **229** (2017), 482–488.
27. A. Hussanan, S. Aman, Z. Ismail, M. Z. Salleh, B. Widodo, *Unsteady natural convection of sodium alginate viscoplastic Casson based nanofluid flow over a vertical plate with leading edge accretion/ablation*, Journal of Advanced Research in Fluid Mechanics and Thermal Sciences **45**(1) (2018), 92–98.

28. A. Hussanan, M. Z. Salleh, I. Khan, *Microstructure and inertial characteristics of a magnetite ferrofluid over a stretching/shrinking sheet using effective thermal conductivity model*, Journal of Molecular Liquids **255** (2018), 64–75.
29. M. Z. Swalmeh, H. T. Alkasasbeh, A. Hussanan, M. Mamat, *Heat transfer flow of Cu-water and Al_2O_3-water micropolar nanofluids about a solid sphere in the presence of natural convection using Keller-box method*, Results in Physics **9** (2018), 717–724.
30. R. Nazar, N. Amin, I. Pop, *Free convection boundary layer on an isothermal horizontal circular cylinder in a micropolar fluid*, Proceedings of Tweifth International Heat Transfer Conference, Paris, Elsevier, **2** (2002), 525–530.
31. J. D. Merkin, (1976) *Free convection boundary layer on an isothermal horizontal cylinder*, American Society of Mechanical Engineers and American Institute of Chemical Engineers, Heat Transfer Conference, St. Louis, MO, August 9–11, 1976.
32. M. A. Mansour, M. A. El-Hakiem, S. M. E. Kabeir, *Heat and mass transfer in magnetohydrodynamic flow of micropolar fluid on a circular cylinder with uniform heat and mass flux*, Journal of Magnetism and Magnetic Materials **220** (2000), 259–270.
33. N. Abbas, S. Saleem, S. Nadeem, A. A. Alderremy, A. U. Khan, *On stagnation point flow of a micro polar nanofluid past a circular cylinder with velocity and thermal slip*, Results in Physics **9** (2018), 1224–1232.

УТИЦАЈ МИКРО-РОТАЦИЈЕ И МИКРО-ИНЕРЦИЈЕ НА НАНОФЛУИДНИ ТОК ПРЕКО ГРЕЈАНОГ ХОРИЗОНТАЛНОГ КРУЖНОГ ЦИЛИНДАРА СА СЛОБОДНОМ КОНВЕКЦИЈОМ

Резиме. Додавање наночестица у конвенционалне течности за пренос топлоте једна је од савремених научних техника које нуде боље перформансе преноса топлоте. Међутим, микрополарни модел течности под овим утицајима наночестица није разматран. Стога је главни циљ овог истраживања проучавање нанофлуида како би се разумела микроструктура и инерцијалне карактеристике наночестица. У овом раду се истражује проток преноса топлоте микрополарне смеше нанофлуида који садржи наночестице бакра (Cu) и сребра (Ag) преко загрејаног хоризонталног кружног цилиндра. Бездимензионалне управљачке једначине решавају се путем имплицитне шеме коначних разлика познате као Keller-box метода. Резултати мешавине нанофлуида упоређују се са резултатима са Њутоновом течношћу. Утицај различитих параметара на брзину, угаону брзину и температуру графички се испитује и за Cu/Ag-воду и за Cu/Ag-керозин. Резултати показују да је коефицијент преноса топлоте смеше нанофлуида Cu/Ag-керозина већи од коефицијента нанофлуида Cu/Ag-вода, када се поређење заснива на фиксној вредности параметра микро-ротације.

Faculty of Informatics and Computing
Universiti Sultan Zainal Abidin (Kampus Gong Badak)
Kuala Terengganu
Terengganu, Malaysia;

Faculty of Arts and Sciences
Aqaba University of Technology
Aqaba, Jordan
mohd12010@yahoo.com

Department of Mathematics
Faculty of Science
Ajloun National University
Ajloun, Jordan

Division of Computational Mathematics and Engineering
Institute for Computational Science
Ton Duc Thang University
Ho Chi Minh City, Vietnam;

Faculty of Mathematics and Statistics
Ton Duc Thang University
Ho Chi Minh City, Vietnam
abidhussanan@tdtu.edu.vn (corresponding author)

Faculty of Informatics and Computing
Universiti Sultan Zainal Abidin (Kampus Gong Badak)
Kuala Terengganu
Terengganu, Malaysia

(Received 20.11.2018.)
(Revised 18.04.2019.)
(Available online 08.11.2019.)